ELSEVIER

Carbohydrate Research 314 (1998) 65–77

CARBOHYDRATE RESEARCH

Synthesis and liquid-crystalline properties of novel archaeal diether-type glycolipids possessing one or two furanosyl units

Rachel Auzély-Velty [a], Thierry Benvegnu [a,*], Grahame Mackenzie [b], Julie A. Haley [b], John W. Goodby [b,1], Daniel Plusquellec [a]

[a] *Laboratoire de Chimie Organique et des Substances Naturelles, associé au CNRS, Ecole Nationale Supérieure de Chimie de Rennes, avenue du Général Leclerc, F-35700 Rennes, France*

[b] *Department of Chemistry, Faculty of Science and the Environment, University of Hull, Hull HU6 7RX, UK*

Received 23 September 1998; accepted 29 October 1998

Abstract

Archaeal diether-type analogues possessing one or two furanosyl polar head groups and methyl branched aliphatic moieties were synthesized by glycosylation of glycerolipids with pent-4-enyl 2,3,5,6-tetra-*O*-acetyl-D-glycofuranosides as the donors. The products were shown to form thermotropic and lyotropic liquid crystalline mesophases, tubules and vesicles. The self-assembling properties of the compounds prepared were found to be similar to those of naturally occurring materials, in that they exhibited columnar thermotropic mesophases and hexagonal lyotropic phases.

Keywords: Archaebacteria; Diethers; Glycosylation; Furanosides; Lyotropic and thermotropic liquid crystals; Tubules; Vesicles

1. Introduction

The lipids of methanogenic and halophilic Archaebacteria are characterized by high proportions of diether-type components with a 2,3-diphytanyl-*sn*-glycerol backbone [1]. Polar groups at the *sn*-1 position of these lipids include various phosphate derivatives and unusual glycofuranosyl units. In particular, glycosyl head groups in *Methanospirillum hungatei*, a methanogen species, consist of repetitious moieties in which the first sugar attached to glycerol is β-D-galactofuranose (β-Gal*f*) and the second one is either β-Gal*f* or α-D-glucopyranose [2]. The presence of β-D-galactofuranose is a striking feature since D-galactose, as well as other hexoses, appears only in the pyranose form in mammalian glycolipids and glycoproteins [3]. Some model diether-type amphiphiles have already been synthesized in order to investigate their ability to form stable vesicles or planar membranes in water [4]. The synthetic molecules contain either straight alkyl chains or phytanyl residues linked to glycerophosphate derivatives. Upon sonication, these compounds furnish well-defined liposomes that are useful for the storage of inorganic salts and proteins with long-term stability and thermostability [5–7]. No study, however, has faced the precise role of furanosyl sugars in archaeal membranes. Here, we describe the synthesis and the evaluation of the liquid-crystalline properties of diether-type glycolipids bearing one or two furanosyl units. Some preliminary results in the preparation of monosaccharidic diethers were recently published [8]. We now report, with full experimental details, the synthesis of a new range of archaeal analogues and the study of their thermotropic and lyotropic mesomorphic behaviour.

* Corresponding author. Fax: +33-2-99-871348.

E-mail address: thierry.benvegnu@ensc-rennes-fr (T. Benvegnu)

[1] Also corresponding author.

0008-6215/98/$ - see front matter
PII: S0008-6215(98)00291-2

2. Results and discussion

Synthesis of glycolipids.—The functional role of polar glycofuranosyl residues in natural membranes is difficult to assess, mainly due to the absence of sufficient information concerning the effects of hexofuranose rings on the physical properties of the resulting archaeal glycolipid–water systems. Although many investigations pertaining to the supramolecular organization of glycerophosphate and glyceroglycopyranoside diethers have been undertaken [4–6], studies on the combined effects of: (i) glycofuranosyl structure: (ii) stereochemistry of the glycerol backbone: and (iii) the length and nature of the hydrocarbon chains are less common [9]. Within this context, we describe an efficient route to the novel diether analogues **1**–**7** possessing: (i) either one or two furanosyl units as polar head groups, namely β-D-galactofuranose, β-D-glucofuranose, α-D-mannofuranose and 6-*O*-β-D-galactofuranosyl-β-D-galactofuranose; (ii) optically pure (*R* or *S*) or racemic glycerol isomers; and (iii) phytanyl, dihydrocitronellyl and/or straight alkyl chains.

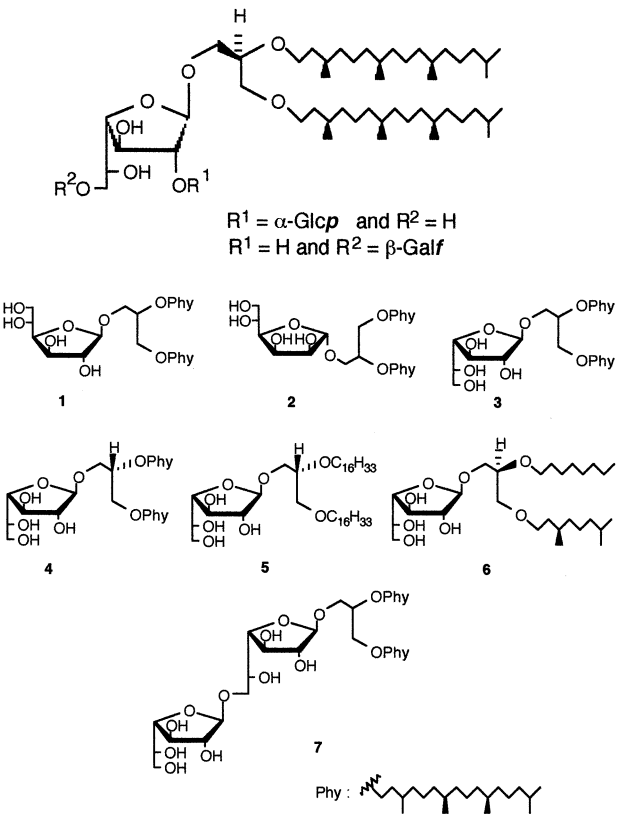

The general synthetic pathway to compounds **1**–**7** involved the preparation of suitable diether-type alcohols **8**–**11** followed by their glycosylation with an appropriate furanosyl donor derived from D-galactose, D-glucose or D-mannose. Synthesis of the known 1,2-di-*O*-alkyl-*rac*-glycerol **8** and 1,2-di-*O*-*sn*-glycerol **9**–**10** bearing either (3*RS*, 7*R*, 11*R*)-dihydrophytyl or hexadecyl chains was accomplished from 3-*O*-benzyl-*sn*-glycerol under classical Williamson conditions [4]. In the case of the glycerol derivative **11**, another strategy was developed to introduce two different alkyl segments, i.e., a dihydrocitronellyl residue and a less bulky octyl chain. (*S*)-1-*tert*-Butyldiphenylsilyl glycidol was readily converted into 3-*O*-[(*R*)-3,7-dimethyloctyl]-1-*O*-(*tert*-butyldiphenylsilyl)-*sn*-glycerol (**12**) via a borontrifluoride etherate-catalysed opening of the oxirane ring with (*R*)-3,7-dimethyloctan-1-ol [10] (68% yield). Alkylation at the C-2 position by octyl triflate [10] proceeded efficiently (60%) in CH_2Cl_2 by heating at reflux for 48 h and using 1,8-bis(dimethylamino)naphthalene (PS) as a base [11]. Removal of the silyl group with tetrabutylammonium fluoride yielded the chiral alcohol **11** in 83% yield.

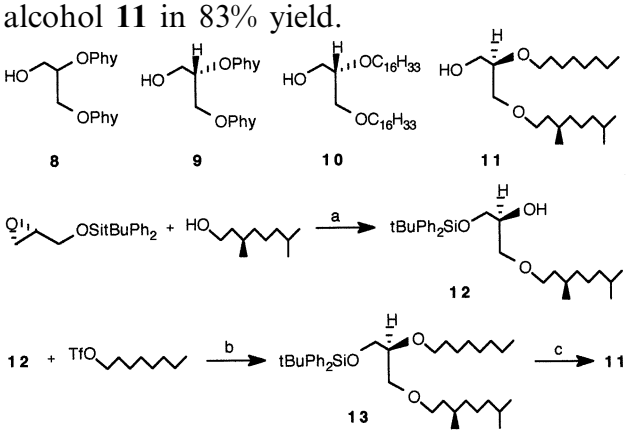

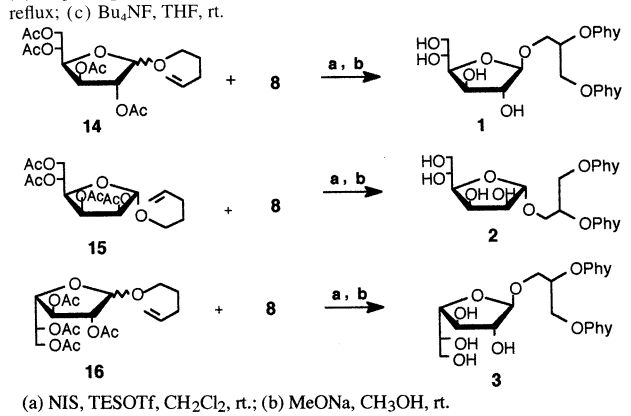

Table 1
Yields of glycosylation and deacetylation, optical rotation values and results of elemental analyses for diethers **1**–**6**

Yield (%)			R_f value[a]	$[\alpha]_D^{20}$ [b]	Elemental	Analysis (%)[c]
Compound	Glycosylation	Deprotection			C	H
1	55	89	0.52		72.09(72.19)	12.23(12.11)
2	82	90	0.60		72.02 (72.19)	12.44 (12.11)
3	75	92	0.62		71.96 (72.19)	12.45 (12.11)
4	69	89	0.62	−29.2	71.99 (72.19)	12.34 (12.11)
5	74	64[d]	0.54	−35.4	70.32 (70.04)	12.13 (11.76)
6	75	90	0.44	−48.9	63.65 (64.00)	10.94 (10.74)

[a] Silica Gel 60 F_{254} non-activated plates (E. Merck) were used. The developing solvent system is CH_2Cl_2–CH_3OH (9:1 v/v).
[b] *c* 1.0 in CH_2Cl_2–CH_3OH (2:3 v/v).
[c] The calculated values of the elemental analyses are shown in brackets.
[d] Yield after recrystallization of **5** in CH_2Cl_2–CH_3OH.

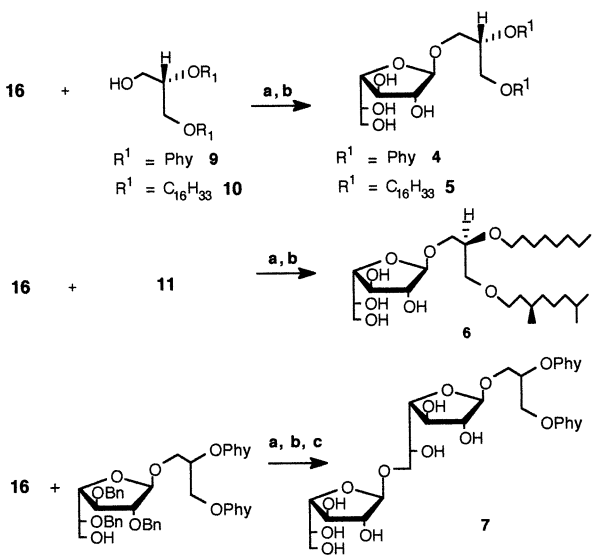

(a) NIS, TESOTf, CH_2Cl_2, rt.; (b) MeONa, CH_3OH, rt.; (c) Pd-C, H_2, CH_3OH-H_2O.

Subsequent introduction of the furanosyl unit on the diethers **8**–**11** was achieved by *n*-pentenyl glycoside (NPG) glycosylation [12]. The key glycofuranosyl donors **14**–**16** were prepared, in a one-pot reaction [13], by ferric chloride promoted glycosylations of 4-penten-1-ol with D-glucose, D-mannose and D-galactose followed in situ by acetylation. Additionally, the coupling reaction of the diethers **8**–**11** with glycosyl donors proceeded smoothly and quickly by using standard NPG conditions [12] (NIS, 1.3 equiv, TESOTf, 0.3 equiv with respect to donors) to afford the resulting glycosides in moderate to high yields (Table 1). Conventional deacetylation by sodium methoxide in methanol resulted in effective deprotection of the hydroxy groups to yield, exclusively, the 1,2-*trans* glycofuranosides (Table 1). The low field resonances (δ 109.5–110.1 ppm) observed for the anomeric carbon C-1′ of compounds **1**–**6** were similar to previously published data [13]. Moreover, the values obtained for $J_{1',2'} < 2$ Hz in the gluco- and galactofuranoside series and the $J_{1',2'} = 2.6$ Hz determined for the mannofuranoside **2** are indicative of a *trans* relationship between H-1′ and H-2′ (Tables 2 and 3). With the aim of investigating the physical properties of diether-type analogues which are structurally closer to the natural archaeal lipids, we also synthesised the glycerol diether **7** bearing a disaccharide as a polar head group. For this purpose, the monosaccharide diether **3** was transformed into 2,3,5-tri-*O*-benzyl-β-D-galactofuranoside by the application of the classical tritylation–benzylation–detritylation sequence of reactions [13]. By employing the galactofuranosyl donor **16**, the disaccharidic moiety was assembled affording, after additional deprotection steps, the novel (1 → 6)-β-D-galactofuranoside dimer **7** (28% overall yield).

Evaluation of mesomorphic phase behaviour of the diethers.—The transition temperatures and heats of transition for compounds **1**–**6** were determined using differential scanning calorimetry (DSC). In addition, polarized transmitted-light thermal microscopy was used as the primary tool for phase identification, classification and determination of transition temperatures. The enthalpy values and

Table 2
^{1}H NMR (400 MHz) data for the glyceroglycosyl moieties of **1**–**7**

δ (ppm)[a] (J (Hz))										
Compound	Glycosyl unit						Glyceryl moiety[b]			
	H-1′	H-2′	H-3′	H-4′	H-5′	H-6′a, H-6′b	H-1a, H-1b	H-2	H-3a, H-3b	OCH_2
1[c]	5.56 [<1]	4.85	4.93	4.98–5.01	4.79–4.84	4.33–4.37, 4.47–4.50	3.50–3.94	3.50–3.94	3.50–3.94, 4.17–4.23	3.50–3.94
2[c]	5.58 [2.6]	4.63–4.66	4.89–4.91	4.63–4.66	4.80–4.85	4.27 [6.2, 11.2], 4.45 [3.3, 11.2]	3.56–3.87	3.90–3.93	3.56–3.87, 4.10–4.15	3.56–3.87
3[c]	5.58	4.85–4.87	4.99–5.03	4.85–4.87	4.53–4.57	4.30–4.40, 4.30–4.40	3.51–3.88	3.92–3.95	3.51–3.88, 4.15–4.19 [4.4, 9.7]	3.51–3.88
4[c]	5.59 [2.0]	4.87–4.90	5.03 [4.3, 6.5]	4.87–4.90	4.55	4.33–4.42, 4.33–4.42	3.52–3.83	3.92–3.97	3.88 [5.3, 10.0], 4.18 [4.8, 10.0]	3.52–3.83
5[c]	nd[a]	4.79–4.81	4.96 [4.2, 6.2]	4.79–4.81	4.51	4.25–4.35, 4.25–4.35	3.46–3.78	3.90	3.82 [5.4, 10.4], 4.12 [4.9, 10.4]	3.46–3.78
6[c]	5.58 [1.9]	4.85	5.00 [4.1, 6.4]	4.85	4.55	4.34, 4.34	3.83 [5.8, 10.3], 4.17 [4.7, 10.3]	3.92	3.53–3.78	3.53–3.78
7[c,d]	5.65	4.84–4.87	5.02	4.71	4.58–4.63	4.15–4.21, 4.43–4.47	3.55–3.61, 3.70–3.90	3.96	3.70–3.90, 4.15–4.21	3.55–3.61, 3.70–3.90

[a] Recorded in pyridine-d_5 + D_2O; nd, not determined.
[b] For compounds **1**–**5** and **7** glycosyl units are linked to the C-3 carbon of glycerol and for **6** to the C-1 carbon.
[c] For compounds **1**–**4** and **7**: δ CH_3 0.90–0.95, δ CH, CH_2 1.06–1.80; **5**: δ CH_3 0.91, δ CH_2 1.32, δ OCH_2CH_2 1.41; **6**: δ CH_3 0.83–0.91, δ CH, CH_2 1.05–1.43.
[d] Data of the furanosyl non-reducing unit of **7** are: δ H-1″ 5.65, δ H-2″ 4.84–4.87, δ H-3″ 5.02, δ H-4″ 4.90–4.93, δ H-5″ 4.52–4.56, δ H-6a″, H-6b″ 4.30–4.37.

Table 3
^{13}C NMR (100 MHz) data for the glyceroglycosyl moieties of **1–7**

δ (ppm)[a]										
Compound	Glycosyl unit						Glyceryl moiety[b]			
	C-1′	C-2′	C-3′	C-4′	C-5′	C-6′	C-1	C-2	C-3	OCH_2
1[c]	110.06, 110.10	81.77	77.55	82.87, 82.91	71.72	65.08	68.71–71.67	78.37–78.43	68.04, 68.15	68.71–71.67
2[c]	109.58, 109.62	78.13	72.40	81.15, 81.17	71.35	64.88	68.55–71.76	78.47–78.62	68.55–71.76	68.55–71.76
3[c]	109.77, 109.83	83.02	78.42, 78.63	84.91, 84.94	72.42	64.43	68.67–71.78	78.42–78.63	67.94, 68.10	68.67–71.78
4[c]	109.94	83.14	78.72	85.10	72.62	64.58	68.69–71.78	78.45, 78.52	67.98	68.69–71.78
5[c]	109.67	82.90	78.44	84.74	72.25	64.31	70.48*	78.36	67.80	71.64*
6[c]	109.73	83.01	78.60	84.85	72.38	64.39	68.08	78.48	69.94*	70.57*, 71.52*
7[c,d]	109.72	82.73	78.41	85.02	70.52	70.86	68.69–73.38	78.41, 78.47	67.94, 68.18	68.69–73.38

[a] Recorded in pyridine-$d_5 + D_2O$; signals marked with * may be interchanged.
[b] For compounds **1–5** and **7** glycosyl units are linked to the C-3 carbon of glycerol and for **6** to the C-1 carbon.
[c] For compounds **1-4** and **7**: δ CH_3 19.74–22.86, δ CH, CH_2 24.74–37.94; **5**:δ CH_3 14.29, δ CH_2 22.92–32.12; **6**: δ CH_3 14.26–22.82, δ CH, CH_2 22.86–39.43.
[d] Data of the furanosyl non reducing unit of **7** are: δ C-1″ 110.05, δ C-2″ 83.00, δ C-3″ 78.47, δ C-4″ 85.26, δ C-5″ 72.47, δ C-6″ 64.32.

Table 4
Transition temperatures (in °C) and enthalpies (in J/g) for the various transitions exhibited for compounds **1**–**6**

Compound	Microscopy data[a]	DSC data				
		Melting		Clearing		Glass transition
		T	Δ*H*	*T*	Δ*H*	*T*
1	Col_h 64.4 Iso Liq					
2	Col_h 53.9 Iso Liq			54.8	0.77	
3	Col_h 70.0 Iso Liq			69.8	0.82	
4	Col_h 69.6 Iso Liq			63.4	0.80	−54.0
5	Cryst 75.4 Col_h124.8 Iso Liq	73.9	131.53	121.4	1.80	
6	Col_h102.5 Iso Liq			101.6	0.37	−25.7

[a] Cryst, solid; Col_h, liquid crystalline phase; Iso Liq, isotropic liquid.

the transition temperatures determined for diethers **1**–**6** are given in Table 4. It is interesting to note that only glycolipid **5**, bearing two linear (unbranched) saturated chains, exhibits two phase transitions in the DSC which correspond to the melting point and the clearing point, whereas all of the other compounds only exhibit enthalpies associated with their relative isotropization points.

Glycosides **1**–**4** and **6**, which carry branched aliphatic moieties, showed no detectable melting point over an appreciably wide temperature range, i.e., on first heating runs from approximately −25 °C to their clearing points. The lack of a clear-cut melting transition can be explained by the fact that the branching methyl groups hinder the ordered packing of the hydrocarbon tails, which in turn hinders formation of the crystal state. Consequently, materials **1**–**4** and **6** are in the liquid crystal state at room temperature. Cooling runs by DSC show that materials **1**–**3** can be supercooled to well below −50 °C without recrystallisation occurring. For compounds **4** and **6** (where **6** possesses mixed linear and branched chains with an *sn*-2 stereochemistry for the glycerol unit), the situation was found to be slightly more complicated. On cooling, compound **4** was found to have a glass transition at −54 °C and compound **6** a glass transition just below −25 °C. Microscopy studies on compound **6** revealed that it formed a glassy state that retained the same defect and textural morphology as in the liquid-crystalline state. Reheating returned the glassy solid to the liquid-crystal state with the same appearance, indicating that the structure of the self-organised system is retained or frozen into the solid state upon cooling. These simple thermal cycling exercises demonstrate the thermal stability of the self-organised structures, and they may give some insights as to why similar glycolipids are prevalent in extremophilic Archaebacteria.

The clearing point enthalpies for all compounds were found to be relatively small (< 1 J/g) in comparison with the values obtained for carbohydrates substituted with a single lipophilic chain (around 5 J/g [9b]). These results indicate that the thermotropic mesophases of diether-type glycolipids have relatively disordered structures which, in their local appearance, are closer to the amorphous liquid than to the solid state. Thus, it is expected that the aliphatic chains will be appreciably melted, the packing of the carbohydrate residues disordered, and the inter-molecular hydrogen bonding dynamic.

The DSC studies also allow for a comparison to be made between the galactofuranose, glucofuranose and mannofuranose systems. We have demonstrated previously [9a] that molecular anisotropy and availability of hydroxyl groups for intra- and inter-molecular hydrogen bonding are important factors in determining phase behaviour. Generally, it was found that the more linear the molecular shape is, the higher is the degree of molecular anisotropy and the greater is the ability to form hydrogen bonds, which in turn promotes higher clearing temperatures. Thus, the β-galactoside, which has a carbohydrate struc-

ture that is nearest to being linear with respect to the other members of the diether series, has the highest clearing point. Additionally, the similar results obtained for galactosides **3** and **4** show that the liquid crystal properties in this case are insensitive to the stereochemistry of the glyceryl units.

Classifications of the mesophases of the products were made via examination of the defect textures formed, in the polarized transmitted light microscope, on cooling from the amorphous liquid. The mesophases formed were all classified as disordered columnar hexagonal phases (Col_{hd}) [14–16]. Upon cooling slowly from the isotropic phase into the liquid crystal state, fan-like defects [17,18], without any hyperbolic or elliptical lines of optical discontinuity associated with the lamellar smectic state, were observed between crossed polarizers (Fig. 1). The smoothness associated with the fan-like domains indicates that the columnar structure is disordered. In addition to the fan-like domains found in homogeneous preparations, rectilinear lines were found in homeotropic areas of the samples. Conoscopy, however, was not able to provide any insights into the signs of the birefringences of the samples which would have confirmed the structures of the mesophases as being columnar (negative uniaxial) rather than lamellar (positive uniaxial). Nevertheless, the presence of homeotropy confirms that the mesophase formed for each of the materials is uniaxial, the absence of

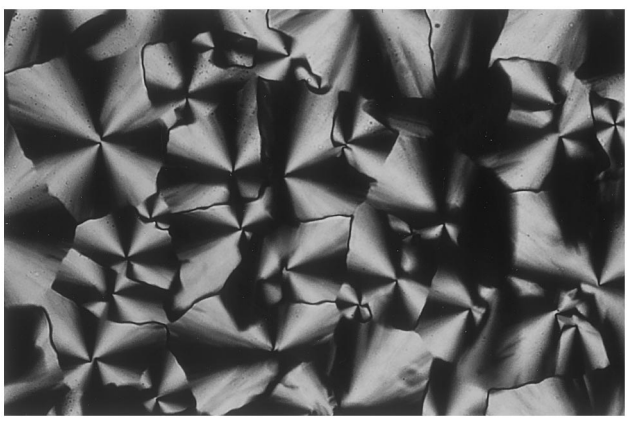

Fig. 1. Typical textures of the columnar hexagonal D_{hd} phase of diethers **1**–**6**, viewed through crossed polarizers, magnification ca. 100X, obtained upon cooling from the isotropic phase.

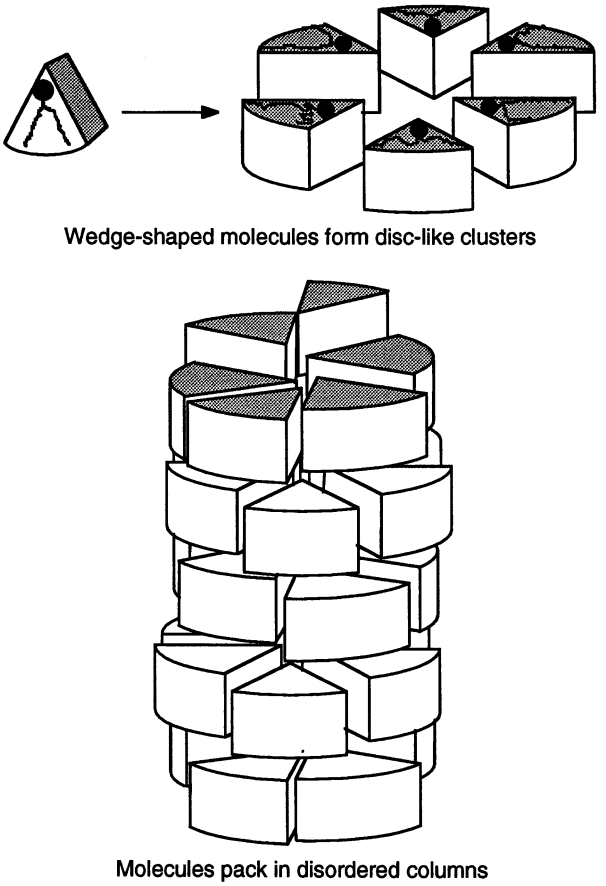

Fig. 2. Schematic representation of the arrangement of glycolipids **1**–**6** in the disordered columnar Col_{hd} phase. The wedge-shaped molecules pack into disc-like clusters, which then self-assemble into columns. There is no periodic order along the column axis.

elliptical and hyperbolic lines of optical discontinuity confirm that the phase is columnar, and the fan-like texture indicates a hexagonal packing of the columns rather than a rectangular packing array.

Turn now to the question why a hexagonal columnar phase is formed by these materials. The molecules have wedge-shaped structures with the polar head groups being towards the apex of the wedge. When the wedge-shaped sugar residues pack together via hydrogen bonding, they will do so apex to apex, thereby forming disordered disk-like clusters. The disc-like aggregates will then stack in columns where the molecules will be disordered along the column axis (Fig. 2), and the columns themselves will pack in a hexagonal array. Thus, the columnar phase will have a structure where the fluid aliphatic chains are towards the exterior of the columns and the

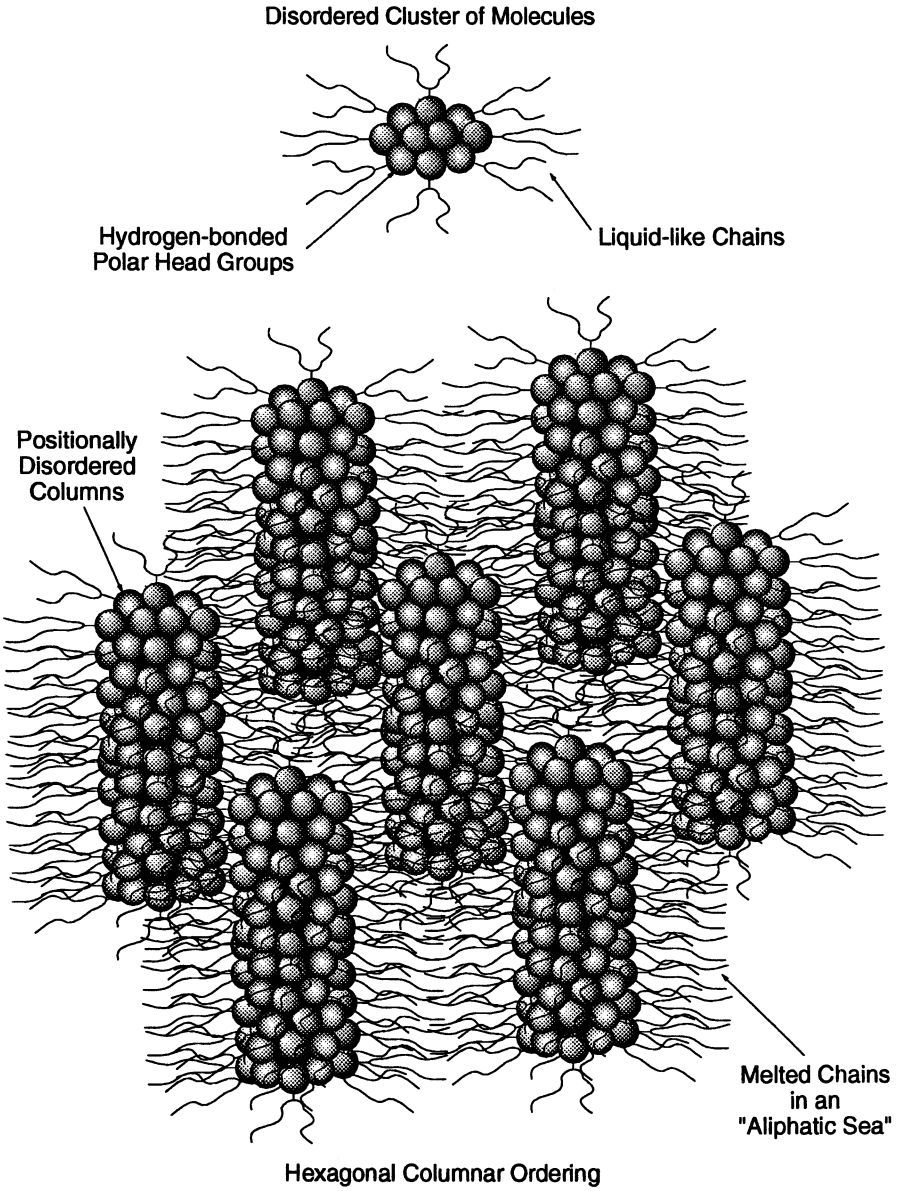

Fig. 3. Schematic representation of the structure of the thermotropic columnar hexagonal phase in which the aliphatic chains are located on the surface and in the exterior of the columns, and the sugar moieties are located towards the inside. The aliphatic chains of neighbouring columns interpenetrate and share space thereby creating a liquid-like 'aliphatic sea' surrounding the sugar columns.

sugar moieties are located in the cores of the columns (Fig. 3). This arrangement of the molecules closely resembles those found in lyotropic H_{II} phases. The observed lack of continuous miscibility of the thermotropic mesophase with water supports the proposed structural model of the phase where the aliphatic chains located on the exteriors of the columns would disfavour water penetration.

The lyotropic phase properties were investigated by simply running a small amount of water onto a crystalline sample of each material sandwiched between a cover-slip and a slide. The solvation process for the materials was then observed in the polarizing microscope. As the thermotropic columnar phases of the materials were not continuously miscible with water at room temperature, lyotropic phase formation for compounds **1**–**6** was observed upon heating the samples. In each case, water penetration into the thermotropic phase did not occur until the clearing point was approached. At the point of the transition to the liquid, the molecular ordering

breaks down and water penetrates immediately resulting in the formation of a hexagonal phase, which for each material exhibited a classical defect texture (Fig. 4). There are two possible structures of the hexagonal lyotropic phase, one where the aliphatic chains are on the inside of the columns and the polar head groups are towards the exterior (i.e. H_I), or alternatively the structure has a double layer arrangement with the polar head groups towards the centre of the column and also on the exterior of the column surface with the aliphatic chains lying in-between.

Self-assembling properties in dilute aqueous media.—The diethers **1**–**7** were sonicated in distilled water at 20–25 °C for 20 min. The ratio of the amphiphiles to the solvent was 1–5 mg/mL. The resulting suspension was centrifuged at 2000*g* for 10 min to give the supernatant, which was then subjected to transmission electron microscopic observation using 2 wt.% aqueous uranyl acetate as a staining agent. The glycolipids were found to self-assemble into various microstructures depending on their structure.

Compounds **1**–**5** containing two identical 16 or 20 carbon atom chains and a monosaccharidic head group exclusively exhibited tubule-like structures of various sizes (Fig. 5(a)). In the case of lipid **6**, which has comparatively shorter hydrophobic aliphatic chains, myelin-type aggregates were produced after sonication (Fig. 5(b)). By contrast, the analysis of dispersions of **7** bearing a more voluminous disaccharidic head group showed the presence of spherical vesicles of 80–500 nm diameter (Fig. 5(c)).

Fig. 4. Lyotropic hexagonal mesophase of diethers **1**–**6**. Photomicrograph of the glycolipid–water interface at 75 °C (top right-neat glycolipid in its liquid phase, bottom left-glycolipid–water soln, centre-lyotropic hexagonal phase): Water has penetrated the isotropic liquid sample to form a band of hexagonal lyotropic phase.

These results clearly indicate that the volumetric ratio of the hydrophilic to the hydrophobic parts plays a major role in the organization of such systems in water. Bulkiness of the disaccharide polar head of the diether **7** brings to the phytanyl chains the degree of freedom apparently necessary for the formation of vesicles. The presence of a decreasing hydrophilic domain favours the formation of elongated cylindrical structures. These aggregates made by the wedge-shaped compounds **1**–**5** can be seen as multiple bilayers in the form of tubular vesicles [19,20]. Interestingly, the tubules formed appear to have almost equidistantly separated parallel defect lines running across the long axes of the tubules, see Fig. 5(a). Lines of this nature are usually associated with chirality, and in particular helicity which results from the way chiral molecules pack together. The results suggest that the tubules either have a helical multilayer structure composed of several hundred molecular layers or else they have a periodic defect structure that is based on some form of helicity. Periodic defect structures are well-known in thermotropic liquid crystals, and are often manifested via a competition between the need for the molecules to form a twisted macrostructure and some structural or space limit on their ability to twist, e.g., Blue Phases, TGB Phases, etc. The competition results in a frustration which is relieved by the creation of defects. For the lipid **6**, the length reduction of the alkyl chains entails a decrease in the steric constraints in the hydrophobic part and, therefore, hinders the formation of tubular structures. In fact, the polar and non-polar parts of this rod-shaped material are too small to participate in the stabilisation of vesicular or tubular aggregates. This could justify why the diether **6** self-assembles into myelin-type structures which probably correspond to complex folding of rolled-up multilayers [21].

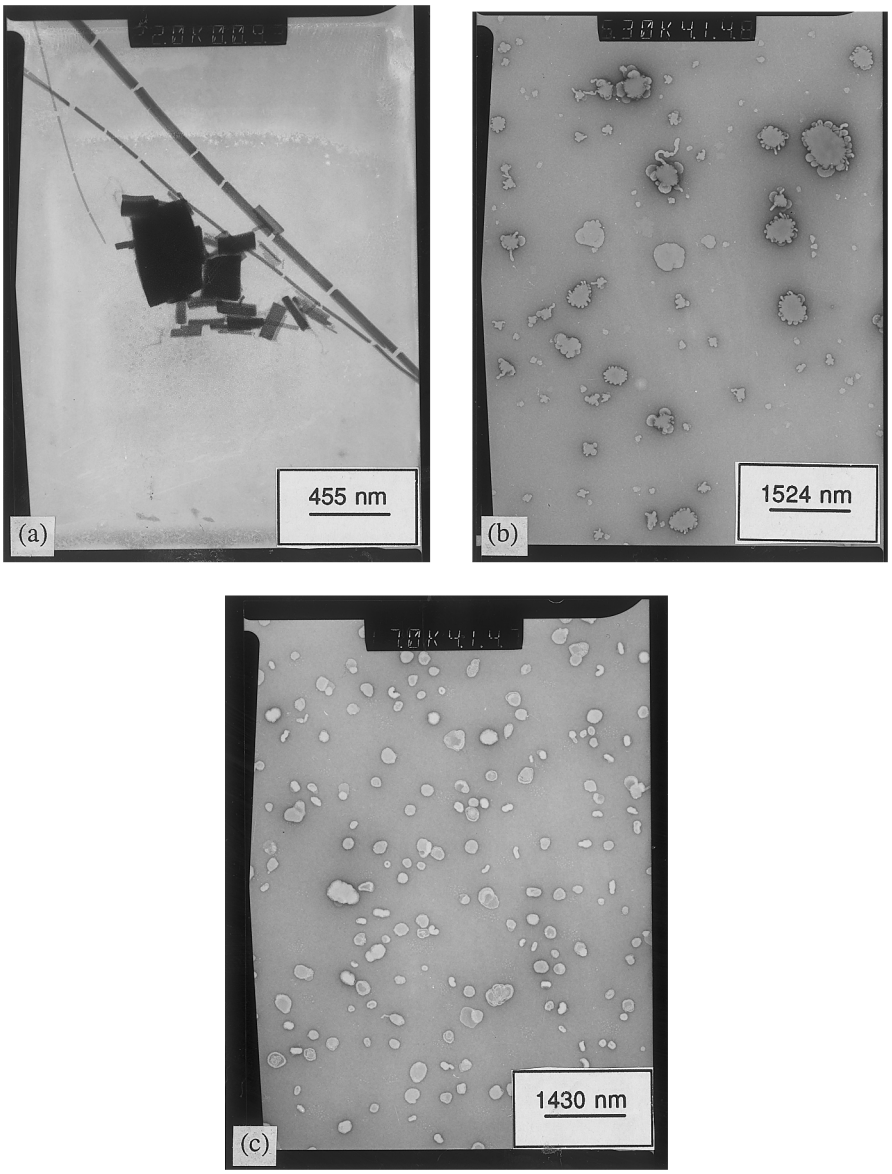

Fig. 5. Electron micrographs of aqueous aggregates of diethers **1**–**7** (stained by uranyl acetate). (a) Tubule-like aggregates obtained from compounds **1**–**4**, (b) myelins from compound **6**, and (c) vesicles from diether **7**.

3. Experimental

Materials and methods.—All reactions were performed under nitrogen in oven-dried glassware. For the coupling reactions, the carbohydrate derivatives were dissolved in a small quantity of toluene and placed under vacuum for 2 h prior to use. Melting points were determined using a Kofler apparatus and are uncorrected. Elemental analyses were made by the Service de Microanalyse de l'ENSCR, Rennes (France). Thin-layer chromatography was performed on $60F_{254}$ Silica Gel non-activated plates (E. Merck). UV light and a solution of 5% H_2SO_4 in EtOH were used to develop the plates. For column chromatography, 60H (5–40 μm) Silica Gel (E. Merck) was used. Optical rotations were measured using a Perkin–Elmer 341 polarimeter. ^1H and ^{13}C NMR spectra were recorded respectively at 400 MHz and 100 MHz using a Bruker ARX 400 spectrometer. Peracetylated *n*-pentenyl glycofuranosides were prepared as previously described [13]. The synthesis of the aliphatic diethers **8**–**10** having two identical chains were carried out according to literature methods [4]. (*R*)-3,7-Dimethyloctan-1-ol was prepared by Raney Ni-catalysed hydrogena-

tion of commercially available (*R*)-(+)-citronellol. The triflate ester of 1-octanol was synthesized as described by Aoki and Poulter [10]. Other chemicals were purchased from Acros or Fluka Chemika. Solvents were of reagent grade and were distilled under N_2 before use: dichloromethane from phosphorus pentoxide, tetrahydrofuran from sodium benzophenone ketyl.

3-O-[(R)-3,7-Dimethyloctyl]-1-O-(tert-butyldiphenylsilyl)-sn-*glycerol* (**12**).—A catalytic amount of $BF_3{\cdot}Et_2O$ (0.04 mL, 0.35 mmol) was added at 0 °C to a solution of (*S*)-1-*tert*-butyldiphenylsilyl glycidol (1.08 g, 3.45 mmol) in dry CH_2Cl_2 (20 mL) under N_2. The resulting mixture was stirred for 17 h at 4 °C before the addition of water (20 mL). The resulting layers were separated and the aq layer was extracted with CH_2Cl_2 (3 × 40 mL). The combined organic layers were washed with satd aq NaCl (30 mL), dried over $MgSO_4$ and solvent was removed under reduced pressure. Purification of the residue by column chromatography (19:1 petroleum ether–EtOAc) afforded **12** (1.10 g, 68%) as a colourless oil; R_f 0.4 (9:1 petroleum ether–EtOAc); ^{1}H NMR ($CDCl_3$): δ 7.68–7.64 (m, 5 H, Ph), 7.45–7.36 (m, 5 H, Ph), 3.92–3.85 (m, 1 H, OCH), 3.70 (d, 2 H, *J* 5.4 Hz, CH_2OSi), 3.53–3.42 (m, 4 H, CH_2OCH_2), 1.65–1.10 [m, 10 H, $CH_2CH(CH_2)_3CH$], 1.06 [s, 9 H, $(CH_3)_3CSi$], 0.87–0.85 (m, 9 H, 3 CH_3); ^{13}C NMR ($CDCl_3$): δ 135.6–127.8 (Ph), 70.7 (OCH), 71.5, 69.9 (CH_2OCH_2), 64.8 (CH_2OSi), 39.3, 37.4, 36.6, 29.9, 24.7 [$CH_2CH(CH_2)_3CH$], 26.8 [$(CH_3)_3CSi$], 22.7, 22.6, 19.7 (3 CH_3), 19.3 [$(CH_3)_3CSi$].

*3-O-[(R)-3,7-Dimethyloctyl]-2-O-octyl-1-O-(*tert-*butyldiphenylsilyl)*-sn-*glycerol* (**13**).—1,8-Bis(dimethylamino)naphthalene (1.20 g, 5.60 mmol) was added under N_2 and at room temperature to a solution of **12** (1.05 g, 2.24 mmol) and *n*-octyl triflate (1.47 g, 5.60 mmol) in dry CH_2Cl_2 (10 mL). The solution was heated at reflux for 48 h. After cooling, the mixture was diluted with CH_2Cl_2 (80 mL), washed successively with 5% aq HCl (30 mL), water (30 mL) and satd aq NaCl (30 mL). The organic phase was dried over $MgSO_4$ and the solvent was evaporated under reduced pressure. The residue was triturated with ether (20 mL) and the ether suspension was filtered through a pad of silica gel. The eluent was removed and the crude product was purified by column chromatography (20:1 petroleum ether–EtOAc) to give **13** (0.79 g, 60%) as a colourless oil; $[\alpha]_D^{20}$ −4.7 (*c* 1.07, CH_2Cl_2); R_f 0.65 (19:1 petroleum ether–ether); ^{1}H NMR ($CDCl_3$): δ 7.70–7.67 (m, 5 H, Ph), 7.44–7.35 (m, 5 H, Ph), 3.71–3.69 (m, 2 H, CH_2OSi), 3.60–3.37 [m, 7 H, $CH(OCH_2)CH_2OCH_2$], 1.63–1.08 [m, 22 H, $CH_2CH(CH_2)_3CH$, $(CH_2)_6$], 1.05 [s, 9 H, $(CH_3)_3CSi$], 0.87–0.85 (m, 12 H, 4 CH_3); ^{13}C NMR ($CDCl_3$): δ 135.6–127.6 (Ph), 79.5 (OCH), 70.7, 70.6, 69.9 (CH_2OCH_2)CH_2OCH_2), 63.6 (CH_2OSi), 39.3, 37.4, 36.7, 31.9, 30.2, 29.9, 29.5, 29.3, 28.0, 26.1, 24.7, 22.7 [$CH_2CH(CH_2)_3CH$, $(CH_2)_6$], 26.8 [$(CH_3)_3CSi$], 22.7, 22.6, 19.7, 14.1 (4 CH_3), 19.3 [$(CH_3)_3CSi$].

3-O-[(R)-3,7-Dimethyloctyl]-2-O-octyl-sn-*glycerol* (**11**).—To a solution of **13** (0.74 g, 1.26 mmol) in dry THF (14 mL) under N_2 a 1.0 M solution of Bu_4NF in THF (2.6 mL, 2.60 mmol) was added. The reaction mixture was stirred for 1 h at room temperature and then water (20 mL) was added. After extraction with ether (3 × 50 mL), the combined organic layers were dried over $MgSO_4$ and concentrated. Purification of the residue by column chromatography (7:3 petroleum ether–ether then ether) afforded **11** (0.36 g, 83%) as a colourless oil; $[\alpha]_D^{20}$ +13.3 (*c* 1.27, CH_2Cl_2); R_f 0.26 (4:1 petroleum ether–ether); ^{1}H NMR ($CDCl_3$): δ, 3.75–3.43 [m, 9 H, $CH_2CH(OCH_2)CH_2OCH_2$], 1.66-1.46 and 1.40–1.06 [m, 22 H, $CH_2CH(CH_2)_3CH$, $(CH_2)_6$], 0.87-0.85 (m, 12 H, 4 CH_3); ^{13}C NMR ($CDCl_3$): δ 78.3 (OCH), 70.7, 70.4, 70.1 [$(CH_2OCH_2)CH_2OCH_2$], 63.1 (CH_2OH), 39.3, 37.3, 36.6, 31.8, 30.1, 29.8, 29.4, 29.3, 27.9, 26.1, 24.7, 22.7 [$CH_2CH(CH_2)_3CH$, $(CH_2)_6$], 22.7, 22.6, 19.7, 14.1 (4 CH_3). Anal. Calcd for $C_{21}H_{44}O_3$: C, 73.20; H, 12.87. Found: C, 73.43; H, 13.01.

General procedure for glycosylation of glycerol diethers and deprotection of tetraacetylated products.—To a solution of the aliphatic diether (0.1 M, 0.8 equiv) and the pentenyl glycoside (1.0 equiv) in dry CH_2Cl_2 at room temperature was added *N*-iodosuccinimide (NIS, 1.3 equiv) followed by triethylsilyl trifluoromethanesulfonate (TESOTf, 0.3 equiv).

The mixture was stirred under nitrogen until TLC analysis indicated complete disappearance of the starting acceptor (10–15 min). Several drops of Et_3N were added to the reaction mixture until it turned into a yellow solution. The resulting solution was diluted with CH_2Cl_2 and washed successively with 10% aq sodium thiosulfate, 0.5% aq HCl (until neutral pH) and satd aq NaCl. The combined organic layers were dried over $MgSO_4$ and the solvent was removed. The crude residue was then subjected to flash column chromatography, using a 9:1 to 4:1 petroleum ether–EtOAc step-gradient mixture, to afford the corresponding tetraacetylated glycolipid. Hydrolysis of the tetraacetylated product (0.20 mmol) with NaOMe in MeOH (2.5 mL) in dry MeOH (0.1 M, 2.5 mL) at room temperature for 2 h gave the crude unprotected diether-type furanosyl lipid which was purified by column chromatography (19:1 CH_2Cl_2–MeOH).

1,2-Di-O-*[(3*RS, *7*R, *11*R*)-dihydrophytyl]-3* - O - *[6* - O - *(β* - D - *galactofuranosyl)* - *β* - D-*galactofuranosyl)*-rac-*glycerol* (**7**).—1,2-Di-*O*-[(3*RS*, 7*R*, 11*R*)-dihydrophytyl]-3-*O*-(β-D-galactofuranosyl)-*rac*-glycerol (**3**) (0.734 g, 0.90 mmol) and DMAP (0.011 g, 0.09 mmol) were dissolved in dry pyridine (10 mL). 4-Anisylchlorodiphenylmethane (MMTrCl) (0.361 g, 1.17 mmol) in dry pyridine (5 mL) was added at 0 °C and the reaction mixture was stirred at room temperature for 72 h. The soln was coevaporated with toluene and the residue was subjected to column chromatography (9:1 CH_2Cl_2–acetone) to afford the corresponding 6-*O*-tritylated compound (0.476 g, 0.44 mmol). To a solution of this compound (0.410 g, 0.38 mmol) in dry DMF (6 mL) was added sodium hydride (60% dispersion in mineral oil, 0.091 g, 2.28 mmol) at 0 °C. After stirring for 15 min, benzyl bromide (0.27 mL, 2.28 mmol) was introduced dropwise. The reaction mixture was stirred for 6 h. Methanol (2 mL) was added and the mixture was evaporated to dryness. The residue was redissolved in CH_2Cl_2 (150 mL), extracted with water (3 × 20 mL) and brine (20 mL), dried ($MgSO_4$), evaporated and chromatographed on silica gel using a 19:1 to 4:1 petroleum ether–Et_2O step-gradient mixture to give the resulting tribenzylated derivative (0.417 g, 0.31 mmol). Part of this oil (0.35 g, 0.26 mmol) was dissolved in AcOH (2 mL) and heated to 70 °C. Water (0.5 mL) was then added dropwise. This soln was stirred at 70 °C for 5 h, coevaporated with EtOH (4 × 5 mL) and chromatographed on silica gel using CH_2Cl_2 and then a 19:1 CH_2Cl_2–acetone mixture to provide the corresponding 6-*O*-deprotected compound (0.195 g, 0.18 mmol) as an oil; R_f 0.28 (7:3 petroleum ether–Et_2O). Glycosylation of this tribenzylated compound (0.148 g, 0.14 mmol) with pentenyl galactofuranoside (**16**) (0.071 g, 0.17 mmol) was achieved following the general procedure previously described. The crude product was purified by flash chromatography using a 3:2 to 2:3 petroleum ether–Et_2O step-gradient mixture to provide the corresponding disaccharide (0.112 g, 0.079 mmol) which was then submitted to Zemplèn conditions (see general procedure). A solution of the resulting deacetylated compound in EtOH–water (2:1, 3 mL) containing 10% palladium on carbon (0.05 g) was stirred under an atmosphere of hydrogen at room temperature for 7 h. The catalyst was removed by filtration on celite and the filtrate was concentrated under vacuum. The residue was chromatographed over silica gel using CH_2Cl_2–CH_3OH (19:1 and then 17:3) to give compound (**7**) [0.039 g, 29% from (**16**)] as a colorless oil; R_f 0.71 (17:3 CH_2Cl_2–CH_3OH). Anal. Calcd for $C_{55}H_{108}O_{13}$: C, 67.58; H, 11.14. Found: C, 67.78; H, 11.26.

Measurements of physical properties.—Phase identifications and determination of phase transition temperatures were carried out, concomitantly, by thermal polarised light microscopy using either a Zeiss Universal or an Olympus BH2 polarized light microscope equipped with a Mettler FP82 microfurnace in conjunction with an FP80 central processor. DSC was used to determine enthalpies of transition and to confirm the phase transition temperatures determined by optical microscopy. Differential scanning thermograms (scan rate 10°/min) were obtained using a Perkin Elmer DSC 7 PC system operating on UNIX software. The results obtained were standardised relative to indium (measured on-

set 156.68 °C, ΔH 28.47 J/g, literature values 156.6 °C, ΔH 28.45 J/g [22]). Comparison of the transition temperatures determined by optical microscopy and DSC show some slight discrepancies. This is due to two factors; firstly, the two methods used separate instruments which are calibrated in different ways, and secondly, and more importantly, the carbohydrates tended to decompose very slightly at elevated temperatures and at different rates depending on the rate of heating, the time spent at an elevated temperature and the nature of the supporting substrate, i.e., the materials decomposed more quickly in aluminium DSC pans than on glass microscope slides.

Studies on the lyotropic phase behaviour of the compounds was carried out by mounting a small amount (~ 10 mg) of each material on a microscope slide, covering it with a cover slip, and then inserting water under the cover slip by way of a syringe. The material was then observed upon heating as it slowly dissolved into the water via the formation of lyotropic phases.

Ultrasonication was performed using a probe-type ultrasonic disintegrator (Vibracell 72412). The transmission electron microscope was a Philips CM-2 with an accelerating voltage of 80 kV.

Acknowledgements

We are grateful to the CNRS and the Region Bretagne for a grant to R.V.; to M. Lefeuvre and C. Penverne for assistance, respectively, in NMR experiments and microanalyses. We also thank J.P. Rolland and D. Thomas for electron microscopic analyses.

References

[1] (a) G.D. Sprott, *J. Bioenerg. Biomembr.*, 24 (1992) 555–566. (b) M. Kates, *J. Microbiol. Methods*, 25 (1996) 113–128. (c) K. Yamauchi, M. Kinoshita, *Prog. Polym. Sci.*, 18 (1993) 763–804.
[2] (a) S.C. Kushwaha, M. Kates, G.D. Sprott, I.C.P. Smith, *Biochim. Biophys. Acta*, 664 (1981) 156–173. (b) M. Tomoaia-Cotisel, E. Chifu, J. Zsako, A. Mocanu, P.J. Quinn, M. Kates, *Chem. Phys. Lipids*, 63 (1992) 131–138.
[3] M. De Arruda, W. Colli, B. Zingales, *Eur. J. Biochem.*, 182 (1989) 413–419.
[4] (a) K. Yamauchi, K. Doi, M. Kinoshita, F. Kii, H. Fukuda, *Biochim. Biophys. Acta*, 1110 (1992) 171–177. (b) K. Yamauchi, K. Doi, M. Kinoshita, *Biochim. Biophys. Acta*, 1283 (1996) 163–169.
[5] E.L. Chang, *Biochim. Biophys. Res. Commun.*, 202 (1994) 673–679.
[6] (a) K. Yamauchi, K. Doi, Y. Yoshida, M. Kinoshita, *Biochim. Biophys. Acta*, 1146 (1993) 178–182. (b) K. Yamauchi, K. Togawa, M. Kinoshita, *Bull. Chem. Soc. Jpn.*, 66 (1993) 2097–2100.
[7] K. Tomioka, F. Kii, H. Fukuda, S. Katoh, *J. Immunol. Methods*, 176 (1994) 1–7.
[8] R. Velty, T. Benvegnu, D. Plusquellec, *Synlett*, (1996) 817–819.
[9] see for example. (a) D. Blunk, K. Praefcke, V. Vill, in D. Demus, J.W. Goodby, G.W. Gray, H.W. Spiess, V. Vill (Eds.), *Handbook of Liquid Crystals*, vol. 3, Wiley–VCH, Weinheim, 1998, pp. 305–340. (b) J.W. Goodby, J.A. Haley, G. Mackenzie, M.J. Watson, D. Plusquellec, V. Ferrières, *J. Mater. Chem.*, 5 (1995) 2209–2220.
[10] T. Aoki, C.D. Poulter, *J. Org. Chem.*, 50 (1985) 5634–5636.
[11] D.H. Thompson, C.B. Svendsen, C. Di Meglio, W.C. Anderson, *J. Org. Chem.*, 59 (1994) 2945–2955.
[12] B. Fraser-Reid, U.E. Udodong, Z. Wu, H. Ottoson, J.R. Merritt, C.S. Rao, C. Roberts, R. Madsen, *Synlett*, (1992) 927–942.
[13] R. Velty. T. Benvegnu, M. Gelin, E. Privat, D. Plusquellec, *Carbohydr. Res.*, 299 (1997) 7–14 and Refs. therein.
[14] Y. Bouligand, *J. Phys.* (*Paris*), 41 (1980) 1307–1315.
[15] S. Chandrasekhar, G.S. Ranganath, *Rec. Prog. Phys.*, 53 (1990) 57–84.
[16] M. Sugiura, M. Mimoda, T. Fukuda, T. Miyamoto, J. Watanabe, *Liq. Cryst.*, 12 (1992) 603–611.
[17] G. Friedel, *Ann. Phys.*, 18 (1922) 273–472.
[18] G.W. Gray, J.W. Goodby, *Smectic Liquid Crystals; Textures and Structures*, Leonard Hill, Philadelphia, 1984.
[19] J.H. Fuhrhop, W. Helfrich, *Chem. Rev.*, 93 (1993) 1565–1582.
[20] J.M. Schnur, *Science*, 262 (1993) 1669–1675.
[21] I. Sakura, T. Suzuki, S. Sakurai, *Biochim. Biophys. Acta*, 985 (1989) 101–105.
[22] R.C. Weast (Ed.), *CRC Handbook of Physics and Chemistry*, 68th ed., CRC Press, Boca Raton, FL, 1988.